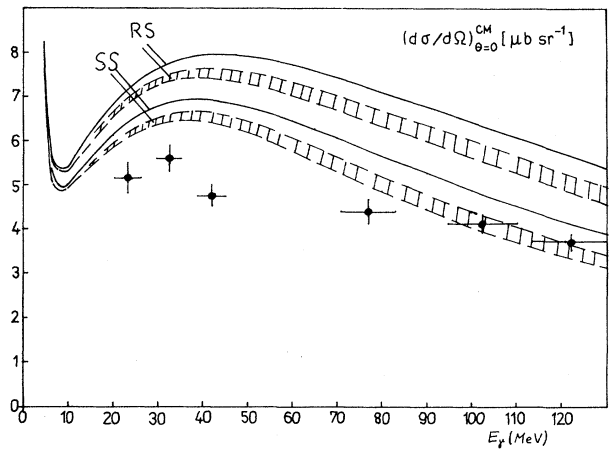

FIG. 3. Full photodisintegration cross section ($\theta = 0°$) including electric and magnetic transitions up to octupole. All retardation effects are included. Meson-exchange contributions to the magnetic transitions are not included. The full curves denote the complete impulse-approximation results for two *NN* potentials: (RS) Reid soft-core and (SS) supersoft core. The dashed curves give the results when the two-body density is included in the calculation of the electric transitions. The shaded areas denote the uncertainties from our present knowledge of the two-body charge density. The experimental data are taken from Ref. 10.

the corrections are even larger. Concerning the charge density it seems worthwhile and necessary to determine this quantity by experiments. Electron-scattering processes (charge scattering) as well as selected electric dipole transitions are good candidates.

Conclusively we remark that the existence of electric two-body operators in the long-wavelength limit has consequences also for other electromagnetic operators such as the Sachs moment, for example.

This work was supported by the Deutsche Forschungsgemeinschaft.

[1]D. O. Riska and G. E. Brown, Phys. Lett. 38B, 193 (1972).
[2]A. J. F. Siegert, Phys. Rev. 52, 787 (1937).
[3]R. Sachs, *Nuclear Theory* (Addison-Wesley, London, 1953); L. L. Foldy, Phys. Rev. 92, 178 (1953); R. G. Sachs and N. Austern, Phys. Rev. 81, 705 (1951). For a recent review see J. I. Fujita and M. Ichimura, in "Mesons in Nuclei," edited by D. Wilkinson and M. Rho (to be published).
[4]J. S. Levinger and H. A. Bethe, Phys. Rev. 78, 115 (1950).
[5]M. Gari and H. Hyuga, Nucl. Phys. A264, 409 (1976), and Phys. Rev. Lett. 36, 345 (1976), and Z. Phys. A277, 291 (1976).
[6]J. Friar, Phys. Lett. 59B, 145 (1975), and to be published.
[7]H. Hyuga and M. Gari, Nucl. Phys. A274, 333 (1976).
[8]M. Gari, H. Hyuga, and J. G. Zabolitzky, Nucl. Phys. A271, 365 (1976); W. Kloet and L. Tjon, Phys. Lett. 49B, 419 (1974); J. Borysowicz and D. O. Riska, Nucl. Phys. A267, 329 (1975).
[9]For a review see Fujita and Ichimura, Ref. 3.
[10]R. J. Hughes, A. Zieger, H. Wäffler, and B. Ziegler, Nucl. Phys. A267, 329 (1976).
[11]H. Arenhövel and W. Fabian, Nucl. Phys. A282, 397 (1977).
[12]M. L. Rustgi, T. S. Sandhu, and O. P. Rustgi, Phys. Lett. 70B, 145 (1977).
[13]E. Lomon, Phys. Lett. 68B, 419 (1977).
[14]R. V. Reid, Ann. Phys. (N.Y.) 50, 411 (1968).
[15]R. de Tourreil and D. W. L. Sprung, Nucl. Phys. A201, 193 (1973).

Role of Particle Transfer and Excitation of Collective Surface Vibrations in the Damping Processes Leading to Deep Inelastic Reactions

R. A. Broglia, C. H. Dasso,[a] G. Pollarolo,[b] and A. Winther
The Niels Bohr Institute, University of Copenhagen, DK-2100 Copenhagen Ø, Denmark
(Received 29 March 1978)

Deep inelastic reactions are studied including both particle transfer and excitations of collective surface modes. Detailed results are given for three examples.

In the collision between two heavy ions the excitation of surface modes is expected to play a very important role.[1-3] In the early stage of the collision especially, the high-lying modes (giant resonances) may absorb an appreciable amount of energy from the relative motion. In the later stage, the dynamics of the surface deformation, as it is determined by the low-lying collective

modes ($\lesssim 6$ MeV), the nuclear surface interaction, and the damping of the vibrational modes, control to a large extent the time scale over which the nuclei interact and the question of whether they eventually will fuse or not.

In earlier calculations we have studied the dynamics of these modes using the surface-surface interaction of proximity type and a spectrum of damped surface modes as determined from nuclear model calculations. The results have confirmed the importance of the surface modes and the necessity of incorporating the mass transfer between the ions.

At the same time theories for the average rate of particle transfer between two nuclei in contact have been developed.[4-7] It has been possible to understand the main features of the distribution of mass in the final products, and to assert the importance of the mass transfer for the energy and angular momentum dissipation. Although the calculations are sensitive to the dynamics of relative motion and deformations, which until now have only been treated in a rather empirical way, it seems difficult to reconcile a complete damping of the energy of relative motion with the observed width of the final mass distribution. Through the simple transfer of particles the ratio of final to initial relative velocity of the two ions during contact is roughly given by $u_f/u_i = \exp(-\Delta m/2m_0)$ where Δm is the total amount of mass exchanged and m_0 is the reduced mass. Since empirically $\Delta m \approx m_0$, the energy loss would be only about half of the available energy.

In this paper we present calculations in which the two aspects of heavy-ion collisions are treated on par.[8]

The surface degrees of freedom are described as discussed in Ref. 2. Both low-lying and giant resonances are included. We assume furthermore that the evolution of the probability distribution for the masses of the interacting ions is governed by a Fokker-Planck equation where the dynamics of the mass transfer is determined by the transport coefficients $\mu_1(A)$ and $\mu_2(A)$.

We utilize the transport coefficients as calculated in the proximity approximation, where

$$\mu_1 = \frac{d\bar{A}}{dt} = 4\pi \bar{R} b \frac{F_A}{T_F} X(s/b), \tag{1}$$

is the mass drift coefficient and

$$\mu_2 = \frac{d\sigma_A^2}{dt} = 4\pi n_0 \bar{R} b \left(\frac{T_a + T_A + |F_A|}{T_F} \right) X(s/b), \tag{2}$$

is the mass diffusion coefficient. They depend on the instantaneous reduced radii of curvature $\bar{R}$, the surface width b, the particle flux n_0 in the bulk of nuclear matter, the mass asymmetry force F_A, the Fermi kinetic energy T_F, and the temperatures T_a and T_A of the two interacting ions.

The effect of the transfer of mass on the relative motion is taken into account by an effective force

$$\vec{F}_{MD} = 4\pi n_0 R b M \{\vec{u} + (\vec{u} \cdot \hat{n})\hat{n}\} \Psi(s/b), \tag{3}$$

where $\vec{u}$ is the relative surface velocity of the two nuclei at the contact point, $\hat{n}$ being a unit vector perpendicular to this surface, and M the nucleon mass. This force acts at the window between the two nuclei. The dimensionless functions $X(s/b)$ and $\Psi(s/b)$ are analogous to the function $\Phi(s/b)$ of the proximity potential[9] (for more details cf. Ref. 7).

In addition to (1) and (2) the equations of motion are

$$\dot{\alpha}_{\lambda\mu}(i) = \Pi_{\lambda\mu}^*(i)/D_\lambda(i), \tag{4}$$

$$\dot{\Pi}_{\lambda\mu}(i) = C_\lambda(i)\dot{\alpha}_{\lambda\mu}(i) - \gamma_\lambda(i)\frac{\Pi_{\lambda\mu}(i)}{D_\lambda(i)} - \left(R_i \frac{\partial U(s)}{\partial r} - \frac{3Z_a Z_A}{(2\lambda+1)} \frac{(R_i^{(0)})^\lambda}{r^{\lambda+1}} \right) Y_{\lambda\mu}^*(\hat{r}), \tag{5}$$

$$\dot{r} = p_r/m_0, \tag{6}$$

$$\dot{p}_r = \frac{1}{m_0}\frac{p_\varphi^2}{r^3} + \frac{Z_a Z_A e^2}{r^2} - \frac{\partial U(s)}{\partial r} + \sum_{\lambda\mu,i} \frac{3Z_a Z_A e^2}{r^2} \left(\frac{\lambda+1}{2\lambda+1} \right) \left(\frac{R_0^{(i)}}{r} \right)^\lambda \alpha_{\lambda\mu}(i) Y_{\lambda\mu}^*(\hat{r}) + f_{MD}(\vec{r}), \tag{7}$$

$$\dot{\varphi} = p_\varphi/m_0 r^2, \tag{8}$$

$$\dot{p}_\varphi = -i \sum_{\lambda\mu,i} \mu \left(R_i^{(0)} \frac{\partial U(s)}{\partial r} - \frac{3Z_a Z_A}{(2\lambda+1)} \frac{(R_i^{(0)})^\lambda}{r^{\lambda+1}} \right) Y_{\lambda\mu}^*(\hat{r}) \alpha_{\lambda\mu}(i) + M_{MD}(\vec{r}), \tag{9}$$

where $f_{MD}(\vec{r})$ and $M_{MD}(\vec{r})$ are the radial force and the torque associated with (3), and $U(s)$ is the proximity potential evaluated at the instantaneous distance s between the surfaces. The quantities $\alpha_{\lambda\mu}(i)$ are the deformation parameters describing the shape of the two nuclei, while $\Pi_{\lambda\mu}(i)$ are the corre-

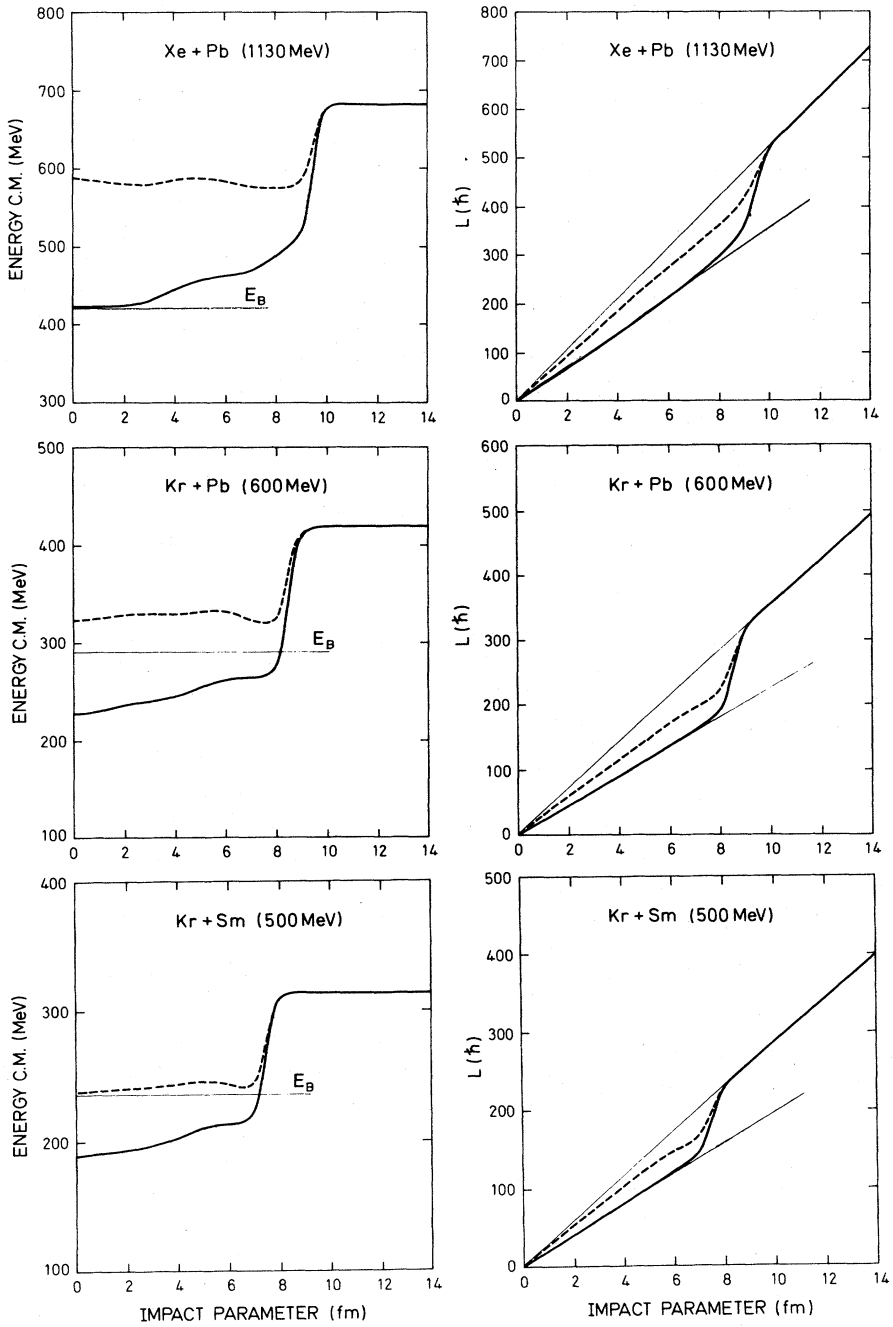

FIG. 1. Exit-channel total kinetic energy and exit-channel angular momentum of relative motion as a function of the impact parameter (entrance-channel angular momentum). For each quantity two curves are given. The dotted curves correspond to dissipated energy and angular momentum through the vibrational modes. The continuous curves correspond to the total dissipated energy and angular momentum, i.e., the sum of the dissipative effects arising from both surface and particle-transfer degrees of freedom. The energy of the Coulomb barrier is indicated in the graphs shown in column I. In the graphs of column II we also display the value

$$l_f = l_i A_a A_A (R_a + R_A)^2 / A_{aA} (R_a + R_A)^2 + \tfrac{2}{5} (A_a R_a^2 + A_A R_A^2)$$

corresponding to the so-called sticking condition, where $A_{aA} = A_a A_a / (A_a + A_A)$. The deflection functions are in all three cases rather similar to the elastic deflection functions (cf., e.g., Ref. 1).

sponding conjugate momenta (fore more details cf. Ref. 2).

The set of coupled equations (1), (2), and (4)-(9) describe the excitation of the low-lying collective surface modes and giant resonance, the transfer of particles in an average way, and the coupling of these degrees of freedom back to the relative motion. About 300–400 coupled equations are integrated for each collision.

In Fig. 1 and Table I we display the predictions of the model for the reactions $^{136}Xe + ^{208}Pb$(1130 MeV), $^{86}Kr + ^{208}Pb$(600 MeV), and $^{86}Dr + ^{144}Sm$ (500 MeV). For all three reactions and for the deep inelastic events, the total kinetic energy in the exit channel is close to or below the Coulomb barrier, in accordance with experiment.[10-13] For the case of the reaction Kr + Pb the maximum angular momentum absorbed by Pb is $\approx 55\hbar$, which compares well with the experimental range of values $(50–80)\hbar$.[14] The calculated full mass width at half-maximum (FWHM) $\Delta_A = 2.4\sigma_A$ is, for both Xe + Pb and Kr + Pb, about 6 amu. For the reaction Xe + Pb the predicted value is to be compared with the experimental range of values[15] 12 amu $< \Delta_A < 23$ amu and the average value of 16 amu.

Concerning the reaction Kr + Pb the experimental situation is somewhat more ambiguous. While the value in Ref. 13 is $\Delta_A \approx 40$ amu for both projectile and target, a rather similar reaction under almost identical bombarding conditions[16] shows a $\Delta_Z \approx 11$ amu (i.e., $\Delta_A \approx 16$ amu) which is consistent with the predicted value.

The predicted average value of the total angular momentum absorbed in the reaction Kr + Sm is $\langle \Delta l \rangle \approx 40\hbar$. This value is compatible with the observed[12] average multiplicity $\langle M \rangle \approx 21$, which corresponds to an angular momentum of about $32\hbar$. The calculated mass FWHM is ≈ 5 amu, to be compared with the experimental value of ≈ 12 amu. Typical energy losses are ≈ 120 MeV which compares well with the predicted values.

The values of σ_A calculated utilizing (2) are systematically smaller than the experimental values. The reasons for this discrepancy are an open problem at present. It is noted that utilizing the prescription of Moretto (cf. Ref. 5) one obtains values of σ_A that are about twice the proximity values, and in rather good agreement with the experiment.

The angular distributions of the deep inelastic events are in all three reactions peaked about the grazing angle (cf. also Ref. 2).

For a detailed comparison with experiments one should consider fluctuations not only in the mass of the fragments but also in the energy and angular momentum loss (cf. Ref. 2), and the influence of these fluctuations on the trajectory.

From the results presented here and from systematic analysis carried out on a variety of reactions, it seems that the excitation of surface vibrations and the transfer of particles play about equally important roles in accounting for the features observed in deep inelastic reactions.

Discussions with P. R. Christensen, O. Hansen, L. Moretto, J. Randrup, and W. Swiatecki are gratefully acknowledged. We are particularly indebted to L. Moretto for clarifications and suggestions.

TABLE I. Energy, angular momentum, and mass transfer widths and drift values for the different reactions at selected impact parameters. The bombarding conditions for Xe + Pb, Kr + Pb, and Kr + Sm are E_{lab} = 1130, 600, and 500 MeV. In columns 1 and 2 the impact parameter (in fm) and the relative angular momentum (in units of $\hbar$) in the entrance channel are reported. In columns 3 and 4 and 7 and 8 the angular momentum (in units of $\hbar$) dissipated through surface modes and through mass transfer are given for both projectile and target, respectively. In columns 5 and 6 and 9 and 10 the energy dissipated (in MeV) through surface modes and through particle transfer are displayed. In the last two columns the mass of the lighter particle and the associated mass standard deviation σ_A (in atomic mass units) are tabulated.

ρ	l_i	l^v	l^m	E^v	E^m	l^v	l^m	E^v	E^m	M_a	σ_A
		^{136}Xe				^{208}Pb					
2	104	6	13	42	71	7	14	60	108	136	5
8	416	21	31	49	35	31	35	54	52	137	2
9	468	23	27	48	26	30	30	51	40	137	2
		^{86}Kr				^{208}Pb					
2	71	3	6	53	31	8	8	43	74	86	4
7	247	17	14	51	19	35	19	48	44	88	3
8	282	24	14	54	14	36	19	46	33	87	2
		^{86}Kr				^{144}Sm					
2	57	2	5	47	23	3	6	26	38	86	3
6	171	12	12	44	14	11	14	24	22	87	2
7	200	18	10	43	10	14	12	26	16	87	2

[a]Present address: Max Planck Institute, Heidelberg, West Germany.

[b]Present address: Istituto di Fisica dell'Università di Torino, Torino, Italy.

[1]R. A. Broglia *et al.*, Phys. Lett. 53B, 301 (1974), and 61B, 113 (1976).

[2]R. A. Broglia *et al.*, Phys. Lett. 73B, 405 (1978).
[3]R. A. Broglia *et al.*, Phys. Rev. Lett. 40, 707 (1978).
[4]W. Nörenberg, Phys. Lett. B52, 289 (1974), and J. Phys. (Paris), Colloq. 37, C5-141 (1976), and references therein; D. Agassi *et al.*, Ann. Phys. (N.Y.) 107, 140 (1977); H. Weidenmüller, in Proceedings of the International Conference on Nuclear Structure, Tokyo, 1977 (to be published).
[5]L. G. Moretto and R. Schmitt, J. Phys. (Paris), Colloq. 37, C5-109 (1976), and references therein; C. Ngo *et al.*, Nucl. Phys. A267, 181 (1976); W. U. Schröder and J. R. Huizenga, Annu. Rev. Nucl. Sci. 27, 465 (1977), and references therein.
[6]W. J. Swiatecki, Lawrence Livermore Laboratory Report No. LBL-4296, 1975 (unpublished), p. 89; J. Blocki *et al.*, to be published, and references therein; S. E. Koonin and J. Randrup, Nucl. Phys. A289, 475 (1977).
[7]J. Randrup, Nordita Report No. 77/45, 1977 (to be published), and private communication.
[8]In this context compare also the important developments of the time-dependent Hartree-Fock description of heavy-ion reactions [e.g. P. Bonche *et al.*, Phys. Rev. C 13, 1226 (1976); A. Kerman, in Proceedings of the International Conference on Nuclear Structure, Tokyo, 1977 (to be published), and references therein]. Compare also N. Takigawa, "A Simultaneous Treatment of High Lying Vibrational Excitations and of Incoherent Excitations in the Deep Inelastic Collisions between Heavy Ions" (to be published); J. N. De and D. Sperber, Phys. Lett. 72B, 293 (1978).
[9]J. Blocki *et al.*, Ann. Phys. (N.Y.) 105, 427 (1977).
[10]W. U. Schröder *et al.*, Nuclear Structure Research Laboratory, University of Rochester, Annual Report, 1975 (unpublished), p. 164.
[11]R. Vandenbosch *et al.*, Phys. Rev. C 14, 143 (1976).
[12]P. R. Christensen *et al.*, to be published.
[13]A. C. Mignerey *et al.*, to be published.
[14]P. Dyer *et al.*, Phys. Rev. Lett. 39, 392 (1977); P. Back and S. Bjørnholm, to be published.
[15]The predicted energy loss for Xe + Pb in the range of impact parameters leading to deep inelastic processes varies between 183 and 258 MeV. The associated Δ_A are thus to be compared with the experimental values $\Delta_A \approx 1.6\Delta_Z \approx 12$–$23$ amu, where $\Delta_Z = (7.8 \pm 0.3)$–(14.3 ± 0.5) amu is the proton FWHM associated with bins number 7 (energy loss 174 MeV) and 10 (energy loss 274 MeV) (cf. Ref. 12). The corresponding average value defined as $\langle\Delta_Z\rangle = \sum_i \sigma_i \Delta_Z{}^i / \sum_i \sigma_i$ is ≈ 10 amu, which corresponds to an average Δ_A of about 16 amu.
[16]Moretto and Schmitt, Ref. 5.

Stabilization of Toroidal Currents in High-β Plasmas by Surface Magnetic Fields

D. L. Mamas, R. W. Schumacher, A. Y. Wong, and R. A. Breun
Department of Physics, University of California, Los Angeles, California 90024
(Received 29 September 1977)

Without the imposition of a toroidal magnetic field, a toroidal plasma current is sustained whose maximum current density increases linearly with the applied poloidal surface magnetic field strength. Both plasma compression and heating are observed in the main weak-field region, and average $\beta \approx 6\%$ and energy confinement time $\tau \approx 1$ msec have been achieved. This concept significantly increases the β values and the allowable current in toroidal, Ohmically heated plasmas.

A toroidal plasma current is usually guided by a toroidal magnetic field and is further stabilized by a vertical field, both of which permeate the entire plasma. The toroidal magnetic field required to satisfy the Kruskal-Shafranov criterion for current stability is so large that in most toroidal devices $\beta \equiv \frac{3}{2}n(T_e + T_i)(B^2/8\pi)^{-1} \lesssim 1\%$ is achieved. We wish to present a concept and related experimental data to describe how a toroidal plasma current is guided by surface magnetic fields only. The stability of the current does not depend on the toroidal magnetic field, so that operation at very low values of safety factor $q \equiv B_t a/B_p R$ is possible. A large plasma current can be induced to flow in the central weakly magnetized plasma, without affecting the overall stability of the plasma, thus separating the functions of Ohmic heating and plasma confinement. The average favorable curvature of the surface magnetic layer provides the overall stability. Based on our measurements of n, T, and B our calculation indicates that a $\beta \approx 1$ layer exists at the edge of the plasma in the surface magnetic layer and volume-average of β of 6% is achieved.

A toroidal Surmac device (*Sur*face *Ma*gnetic Confinement[1]) has been constructed to test these concepts. A background plasma of initial density 3×10^{13} cm^{-3} and temperature 1 eV injected by a Marshall gun is confined by a toroidal surface magnetic layer of ≈ 500 G, provided by pulsing a

